11th International Workshop on Ship and Marine Hydrodynamic
Hamburg, Germany, September 22-25, 2019

Experimental Investigation of Vortex-Induced Vibrations Using 3D-Accelerometry and Digital Image Correlation

S. Tödter[1,*], H. El Sheshtawy[1], J. Neugebauer[1], O. el Moctar[1]

[1]University of Duisburg-Essen,
Institute of Ship Technology, Ocean Engineering and Transport Systems (ISMT)
Bismarckstraße 69, 47057 Duisburg, Germany

[*]Corresponding author, simon.toedter@uni-due.de

ABSTRACT

Tower structures of wind turbines are often installed in various configurations at the port before being transported by ships. Vortex-induced vibrations may occur when the natural frequency of the structure is close to flow vortex shedding frequency. This leads to a considerable reduction of their fatigue life. The phenomenon is well-known for risers in the oil and gas industry. Here, we present an experimental study of vortex-induced vibrations (VIV) of a fully and partially submerged hollow cylinder in water. A circulating water channel generated the flow towards the test bodies. Two hollow cylinders with a length-to-diameter ratio (l/d) of 28.13 and 18.5 and an outer diameter of 32 mm were used. Each cylinder was equipped with three-dimensional accelerometers. From the acceleration data, a two-fold integration delivered the motion amplitudes of the cylinders at the location of the accelerometer.
In addition, a speckle pattern was applied to the cylinders and captured with two high-speed cameras, arranged in different orientations to the cylinder. Three-dimensional Digital Image Correlation (DIC) was used to measure the motion trajectories for the areas of the cylinder, covered by a speckle pattern. First, decay tests for the test bodies were performed in air and water. From the motion trajectories, the natural frequencies and damping coefficients were evaluated. Second, tests in uniform flow were conducted under fully and partially submerged conditions for different flow velocities. Flow effects such as reduced velocity on vibration were assessed in terms of motion amplitudes and frequencies in longitudinal and transverse direction. The results from DIC and accelerometer measurements were compared and the suitability of DIC for VIV investigations was discussed.

1 INTRODUCTION

In maritime applications, the flow around pipes or cylinders may induce substantial structural vibrations. Owing to the significance of this problem, extensive experimental investigations of flow-induced structural loads have been conducted. However, these phenomena are not completely covered scientifically (Prastianto et al. [1]). Khalak and Williamson [2, 3] designed and developed an experimental procedure to test a rigid cylinder fixed on one end at the top of a flow channel. They measured the displacement, the lift and drag forces for different inlet flow velocities, and Khalak and Williamson [4, 5] used the same procedure to test the behaviour of an elastic cylinder. They measured the forces and the structural displacement.

The structural dynamic of a cylinder in a flow of water is not only influenced by the cylinder elasticity but also the cylinder free end condition – fixed or free to move (Prastianto et al. [1]). Fujarra et al. [6] investigated the dynamic behaviour of an elastomeric material cantilever. The structure was restrained in the flow direction by an thin aluminium plate. The objective was to increase the stiffness in the flow direction compared to the transverse flow direction. The free end of the cantilever was fixed at the top. They

compared their results with the dynamic behaviour of a felixible cantilever, which had the same felxibility in both directions (Fujarra et al. [6]), and a rigid cylinders (Khalak and Williamson [3]). Prastianto et al. [1] measured the dynamic behaviour of a flexible free hanging cantilever in a flow and forces acting on it. The cantilever was mounted vertically and it was clamped at its top. They used the same set-up like Prastianto et al. [7].

Wang et al. [8, 9] studied the effect of vortex-induced vibration (VIV) on a horizontal aligned cylinder, which was fully submerged and was free to move only in the flow transverse direction. The damping parameters were maintained constant. They studied the effects of different flow velocities, and used Particle Image Velocimetry (PIV) to measure the velocities and the related vorticities. Furthermore, they investigated details of the shape and the dynamics of the vortices. Shaharuddin and Darus [10] tested an aluminium pipe (horizontally and vertically orientated) in a small tank and compared their results with the literature. A comprehensive literature review covering findings of experimental and computational studies of VIV of cylinders in water is given in Williamson and Govardhan [11, 12], Sarpkaya [13] and Wu et al. [14].

Helfrick et al. [15] carried out full-field vibration measurements in air using 3D Digital Image Correlation (DIC). Tang et al [16] investigated large deformations during tensile strength trials with 3D DIC, where the main displacement was in-plane. Banks et al. [17] and Bleischwitz et al. [18] measured deformations resulting from fluid-structure interactions (FSI) of an aerofoil during wind channel tests. Gupta et al. [19] studied the deformations resulting from underwater implosions with 3D DIC. Hild and Roux [20] and Pan et al. [21] reviewed the theoretical background of DIC.

In the present work, we performed an extensive experimental study on VIV of a fully and partially submerged hollow cylinder in a water circulation tank. Unlike most of the published studies, the cylinders were free to move at one end and fixed at the circulation tank bottom. First, we measured the accelerations using 3D accelerometers. Integrating the accelerations yields the displacements. Second, we measured the displacement using the optical 3D DIC method. We compared the results of both methods.

2 EXPERIMENTAL PROCEDURE

We performed the experiment in our circulating water channel with a maximum flow velocity of 2.60 m/s. The total depth of the water channel is 670 mm, the width is 1476 mm and the measuring section length is 6000 mm. The two test cylinders were made of polyvinyl chloride (PVC) material. Both hollow cylinders had an outer and inner diameter of 32 mm and 28.6 mm, respectively. The partially submerged cylinder was 900 mm long and the fully submerged cylinder was 600 mm long. The cylinders were mounted at the top of a force-torque-sensor, which was located underneath the moveable tank bottom. A threaded bolt led through the tank bottom and connected the sensor with the cylinder. A 5 mm gap was between the bottom and the cylinder to avoid contact due to deflection and thus influence the cylinder motion. Thus, the partially submerged cylinder had a length-to-diameter ratio (l/d) of 28.125 and a mass ratio (m^*), the mass of the cylinder divided by the mass of the water displaced by the cylinder, of 0.723. The fully submerged cylinder had a l/d of 18.75 and a m^* of 0.556.

Three 3D accelerometers, type Disynet DA 3802−015g, were placed inside the partially submerged cylinder. The upper one was located at the top of the cylinder. Both others were placed in the field of view for the DIC measurements to get comparable results. The filed of view was located at a very low position to avoid an optical influence on the DIC measurements due to ventilation.

For the fully submerged cylinder, one accelerometer was inserted 30 mm below the top. A water-tight cover, which weights 0.019 kg and has an height of 30 mm, was placed at the top of the fully submerged cylinder. Each accelerometer weights 0.015 kg, is 15x15x15 mm in size, and can measure up to 15 gravity (up to 40 gravity over range). The measurement error of the accelerometers is reported to be no more than 0.3 %. Figure 1 depicts the accelerometer arrangements of the fully and partially submerged cylinder.

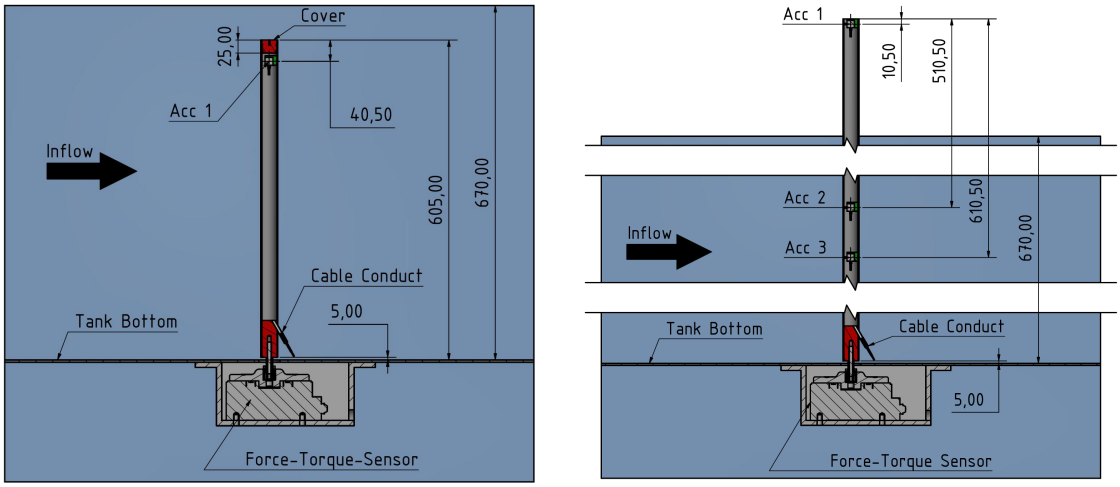

(a) (b)

Figure 1: Accelerometer arrangement of the fully submerged cylinder (a) and the partially submerged cylinder (b)

Figure 2 shows the top view of the partially submerged cylinder. Here, the accelerometers were placed with 3D-printed cylindrical fittings. However, the sensors was 0.6 mm off the cylinder centre in flow direction. The three accelerometer cables were conducted through the cylinder bottom side to avoid effects on the cylinder structural properties. Shrink hoses tightened the conducts against water entry.
Three HBM QuantumX MX840B data amplifiers were used as data acquisition system. The sampling rate was 2400 Hz. The flow velocity was measured locally right in front of the test cylinder using a Schiltknecht MiniWater 20 flowmeter. The flowmeter was removed before the measurements. The measurement error of the flow meter is 2.0 %.

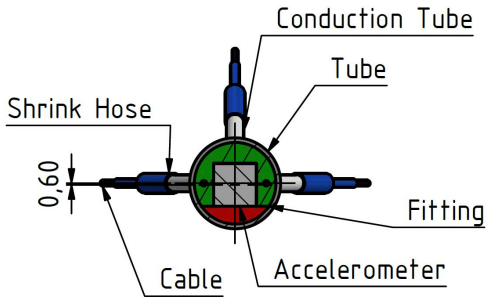

Figure 2: Cylinder cross section

2.1 Optical and Digital Image Correlation Set-Up

Digital Image Correlation (DIC) technique uses a speckle pattern attached to the structure to monitor its displacement. With two captured images, DIC computes the displacement based on the relative pattern shift. Three-dimensional displacements can be detected using more than one camera synchronously. Thus, a dye pattern was attached to the cylinder surface with a porous sponge. Figure 3a shows the applied pattern of the fully submerged cylinder.
Two phantom v9.1 high-speed cameras with an adjusted capture rate of 300 fps were used to capture the 3D pattern shift. The timing and synchronization of both cameras was realized with a high-speed controller, which also synchronised the DIC and accelerometer measurements. The motion was captured for 5 s for every test.
The distance between the cameras and the cylinder was about 1 m for the fully submerged cylinder and

1.2 m for the partially submerged cylinder. The angle between the cameras was 23.7° for both arrangements. The field of view for the fully submerged cylinder was 210 mm x 285 mm, capturing the region around sensor Acc 1, and for the partially cylinder 148 mm x 350 mm, capturing the region around the sensors Acc 2 and Acc 3, see Figure 1. Due to the camera orientations, displacements in flow direction are in-plane and motions normal to the flow out-of-plane.
Four LED headlights, equipped with twelve LEDs each, illuminated the area of interest. The image capturing and digital post-processing was carried out with the software LaVision StrainMaster [22]. Figure 3b shows the optical set-up for the DIC measurement with the LED headlights, both high-speed cameras and the cylinder mounted inside the circulating water channel. Additionally, a dark coated 3 mm Perspex plate was placed inside the tank to avoid reflections at the glass walls and give a uniform image background.

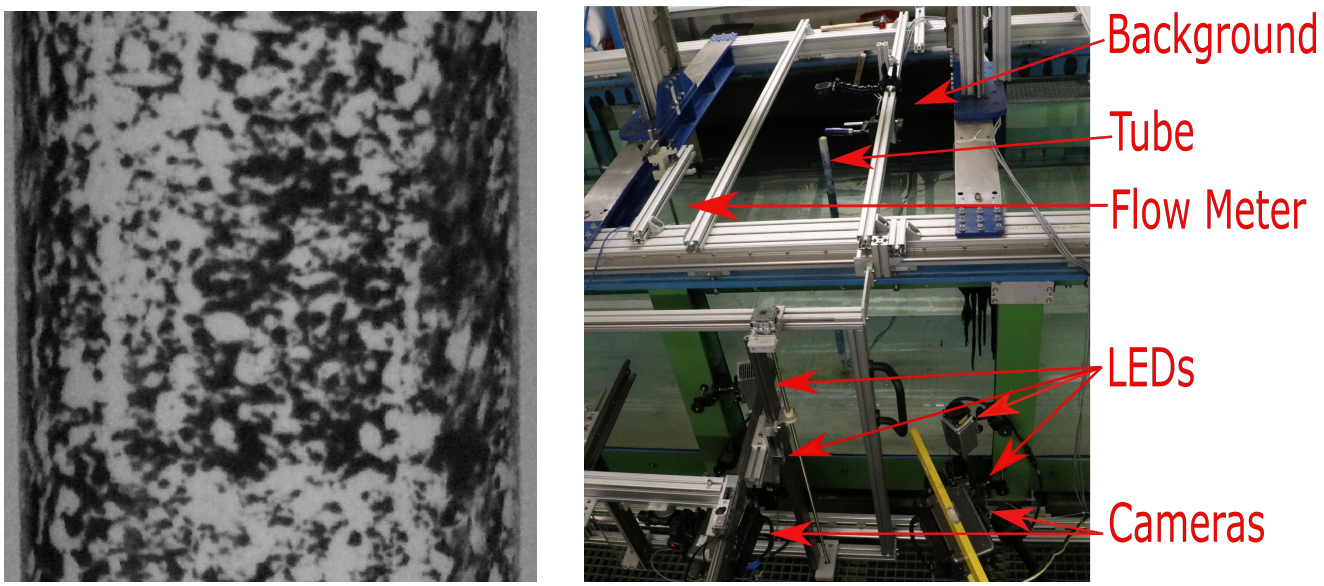

(a) (b)

Figure 3: Applied pattern on the fully submerged cylinder (a) and optical set-up for DIC (b)

3 RESULTS

3.1 Comparative Estimation of Natural Frequencies and Damping Ratios

We performed tests with two different configurations to compute the natural frequency (f_n) and the damping ratio (ζ). First, we carried out hammering tests as shown in Figure 4 for one test case. These tests were repeated ten times in flow and transverse flow directions, each. The tests were performed in air as well as in water. Second, we carried out free decay tests, which were repeated three times, in both directions. The free decay tests were performed using a mechanism, which deflected the cylinder initially, hold it and released it afterwards. For estimation of natural frequencies and damping ratio, the acceleration data was filtered with a low pass filter of 80 Hz to cut off the noise, but meanwhile capture the complete acceleration signal. Figure 4a represents the hammering test and the filtered signal for the fully submerged cylinder. It is shown that, the filtered signal has the same maximum and minimum amplitudes. The Fast Fourier Transformation (FFT) is used for the filtered acceleration signal as shown in Figure 4b and the peak value is located at a frequency of 11.47 Hz, which represents the first natural frequency. Figure 5a shows a sample test case of the acceleration from the free decay test, and Figure 5b its FFT, where the natural frequency is 11.41 Hz.

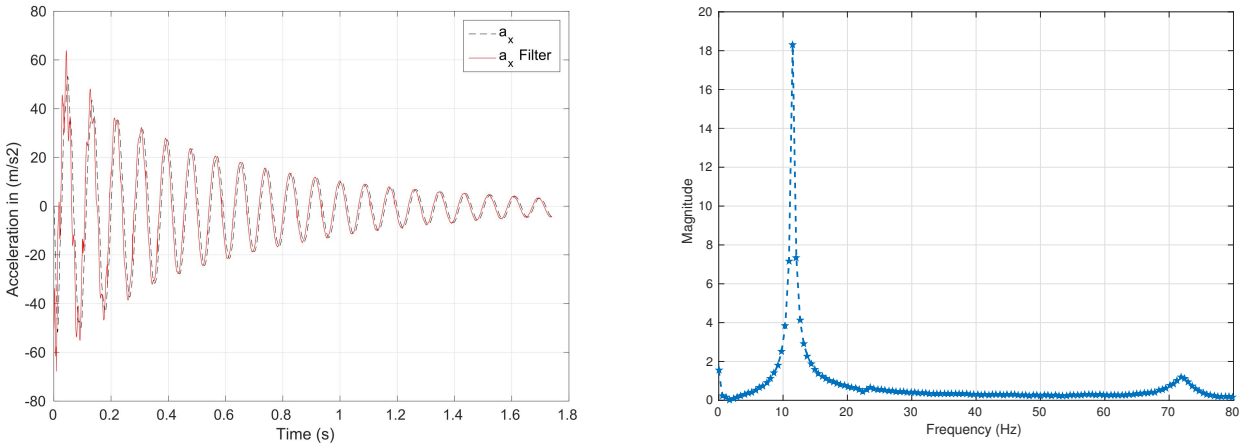

(a) (b)

Figure 4: Hammering test of the fully submerged cylinder (a) and Fast Fourier Transformation of the filtered acceleration (b)

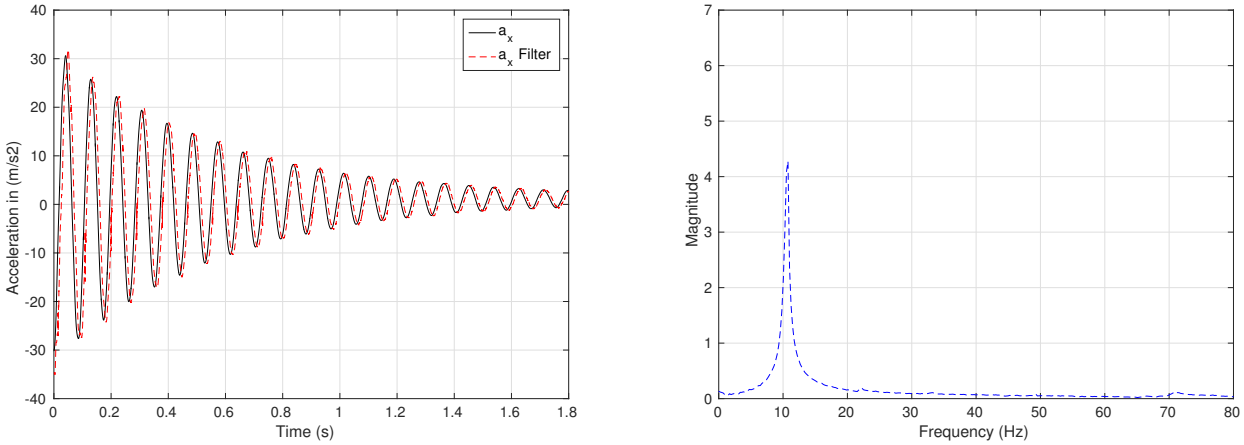

(a) (b)

Figure 5: Free decay test of the fully submerged cylinder (a) and Fast Fourier Transformation of the filtered acceleration (b)

Equation 1 is used to calculate the damping ratio ζ. Therefore, the acceleration is integrated twice to get the displacements.

$$\frac{1}{n} \ln \left(\frac{Y_n}{Y_{n+1}} \right) = \frac{2\pi\zeta}{\sqrt{1-\zeta^2}} \tag{1}$$

Here, Y_n and Y_{n+1} are two successive oscillation peaks, n is the number of the considered peak and ζ is the damping ratio. Figure 6a depicts the left side of Equation 1 vs. its right side for the first twelve peaks of the hammering test shown in Figure 4. The relation is linear, means the system is linear damped and ζ equals 0.01651. Figure 6b does the same for the free decay test shown in Figure 5, and ζ is equal to 0.01598.

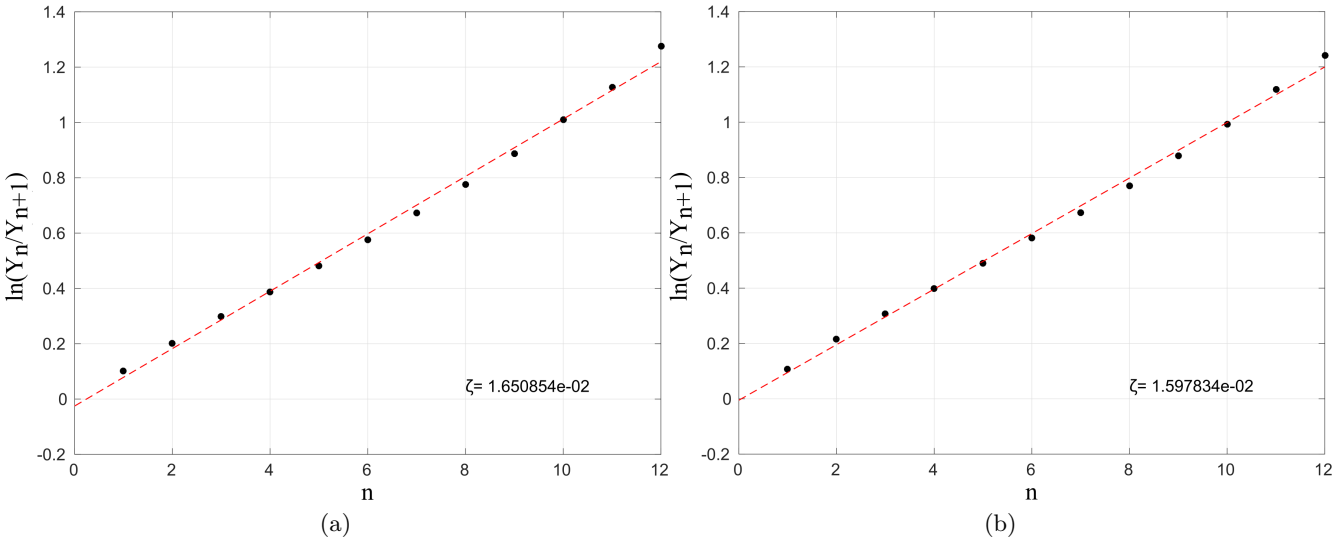

Figure 6: Estimation of the damping ratio ζ of the fully submerged cylinder for one hammering test (a) and for one free decay test (b), where the points are the single amplitudes of the decay and the red line is the curve fitting

As mentioned earlies, the tests were repeated several times. The mean values for all repetitions are displayed in Table 1. For the fully submerged cylinder, the ratio of the natural frequencies f_n in air and water is 1.66 and the ratio of the damping ratios ζ in air and water is 0.4. For the partially submerged cylinder, the the frequency ratio is 1.30 the ratio of damping ratios is 0.79. The comparison shows, that hammering and free decay tests yield similar natural frequencies f_n. However, the damping ratios ζ differ between acceleration and DIC measurements. The reasons may be due to out-of-plane errors related to their estimation.

Table 1: The average values of natural frequencies and damping ratios for the two cylinders by hammering and decay test

Item	Method	f_n, air (Hz)	ζ, air	f_n, water (Hz)	ζ, water
fully submerged	Acc-Hammering	19.06	0.0038	11.470	0.0095
fully submerged	Acc-Free Decay	-	-	11.413	0.0091
fully submerged	DIC-Free Decay	-	-	11.322	0.0150
partially submerged	Acc-Hammering	10.366	0.0119	7.963	0.0151
partially submerged	Acc-Free Decay	-	-	7.713	0.0210
partially submerged	DIC-Free Decay	-	-	7.617	0.0148

The free decay tests were also performed using DIC. Figure 7 depicts comparative accelerometer and the derived DIC results of the fully submerged cylinder for one test case. The DIC values show the same behaviour with a small time delay compared to the accelerometer method However, the displacement amplitudes resulting from DIC are higher than those measure with the accelerometer method.

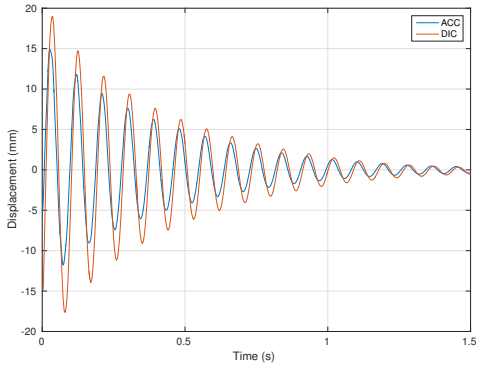

Figure 7: Comparative free decay test of the fully submerged cylinder measured with accelerometer and DIC method

3.2 Comparative Accelerometer and DIC Measurements for Different Flow

The synchronous measurements with DIC and accelerometers allow to compare the results and quantify the suitability of DIC for VIV investigations. Figure 8 plots comparative results of both measurement techniques for the partially submerged cylinder at 1.2 m/s inflow velocity. Part a shows the unfiltered acceleration of accelerometer Acc 2 normal to the flow (y) and the influence of the applied 100 Hz lowpass filter. The filter cuts off the high frequency vibrations and acceleration peaks because they are of minor interest in the present study. The DIC frame rate of 300 fps is to low to capture high frequency vibrations. Therefore, only the dominant low frequency oscillation is compared.
Figure 8b compares the measured acceleration with the derived accelerations from the DIC records. Here, the accelerations in flow direction (x) are relatively small and are of similar amplitude and frequency. The same applies for the oscillation normal to the flow (y-direction). However, the two-fold derivation leads to high frequent noise around the peaks.
Figure 8c depicts the DIC displacement measurements at the surface, where accelerometer Acc 2 is placed, and the displacements through two-fold integration of accelerometer Acc 2. The integrated accelerometer displacements are filtered with a 2 Hz to 100 Hz bandpass filter. Here, the transverse (y) oscillation has the same frequency for both techniques. Nevertheless, the amplitudes differ slightly. The average difference of the normalised transverse amplitude between both methods in the synchronised interval is 4.02 %, which equals 0.20 mm. Figure 8d shows the FFT analysis of both measurement techniques. The progress of the motion amplitude versus the frequency is almost identical above 4.5 Hz for both measurement techniques. Only the peak value differ slightly. Underneath 4.5 Hz the progresses differ strongly but the amplitude values are small compared with the peak. Thus, the influence of this part is comparable low.
The exemplary results show, that for the inflow velocity and the resulting amplitudes the accelerometer and DIC results have a sufficient comparability. Nevertheless, one result does not justify the assessment of the capability of DIC for VIV experiments. Therefore, different reduced velocities ($U^* = U/(f_n \cdot D)$), the normalized ratio between the flow velocity U to the natural frequency of the body f_n and the cylinder outer diameter D, were induced to the cylinder and the dynamic behaviour of the cylinder was measured with accelerometers and DIC. The normalized motion amplitude ($A^* = A/D$), the ratio between the vibrating amplitude A to the outer diameter of the cylinder D, of the cylinder in x and y directions were measured at different U^* and the median amplitudes of the synchronised interval for both measurement techniques are shown in Figure 9.
Figure 9a shows, that up to a reduced velocity of $U^* = 3.27$ the motion amplitude of the fully submerged cylinder (compared at the position of the accelerometer Acc 1) in flow direction is lager than the transverse amplitude and the results of both measurement techniques are almost identical. For $U^* > 3.27$, the result of vibrating motion for the two methods in flow direction were approximately the same. The amplitude normal to the flow start to differ increasingly. However, it follows the same trend up to $U^* = 4.36$, where the deviation is 13.4 %. Above, the amplitudes normal to the flow differ strongly and are not comparable any

more. Higher velocities were not possible to investigate because for $U^* > 5.42$ the amplitude increased, and the fully submerged cylinder was destroyed. Consequently, the experiment of the fully submerged cylinder stopped at $U^* \approx 5.42$.

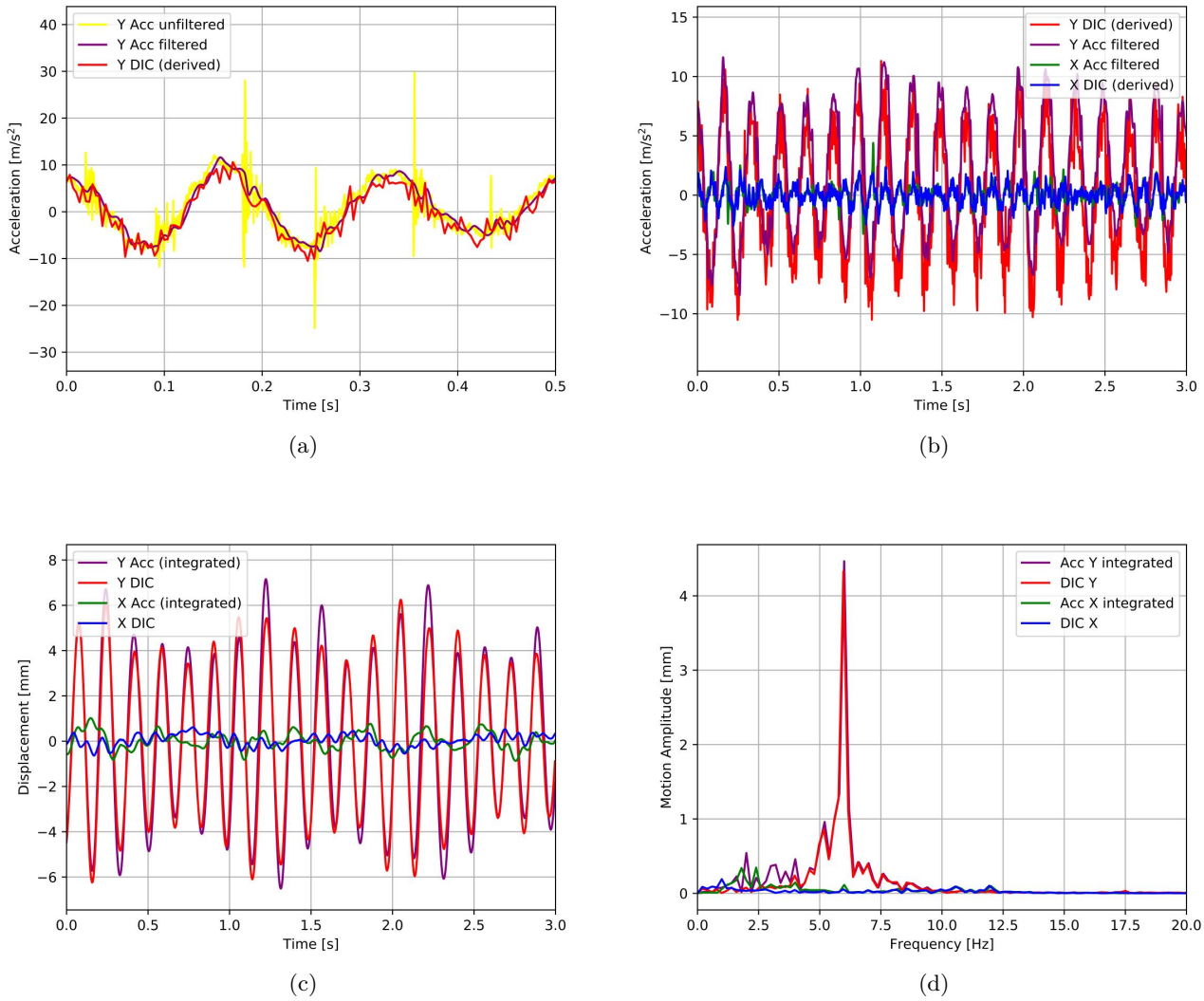

Figure 8: Results of the partially submersed cylinder for 1.2 m/s flow velocity: Filter of acceleration (a), comparative acceleration results (b), comparative displacements (c) and FFTs of both measurement techniques (d)

Figure 9b depicts the normalised motion amplitude versus reduced velocity for the partially submerged cylinder at the position of the accelerometer Acc 2, for which the same experiment was done at a wider range of U^*. For $U^* < 3.1$ the normalised oscillation amplitude A^* in flow direction is larger than normal to the flow. This streamwise branch is typically for cylinders at low mass and damping with two degrees of freedom (Jauvtis and Williamson [23, 24]). The differences between the results of both measurement techniques in flow direction are almost constantly low, except for U^* ranging from 4.8 to 8.33, where the transverse displacement is maximum due to resonance and the displacement in flow direction is comparably small. In flow direction, the differences are first relatively large for U^* ranging up to 3.1, where the amplitude is small. Afterwards, the transverse displacement amplitude becomes dominant and the motion amplitude is almost equal for both methods up to $U^* = 5.24$. Next, the deviations increase

up to $U^* = 7.86$ and decrease afterwards, where the cylinder leaves resonance, but the deviation remains larger then for $3.1 \leq U^* \leq 5.24$.

Figure 9c shows the normalised motion amplitude A^* in flow and transverse direction measured only by the top accelerometer Acc 1 of the partially submerged cylinder. Both curves act likely the curves of Acc 2 but with a larger Amplitude for both directions, which is expected.

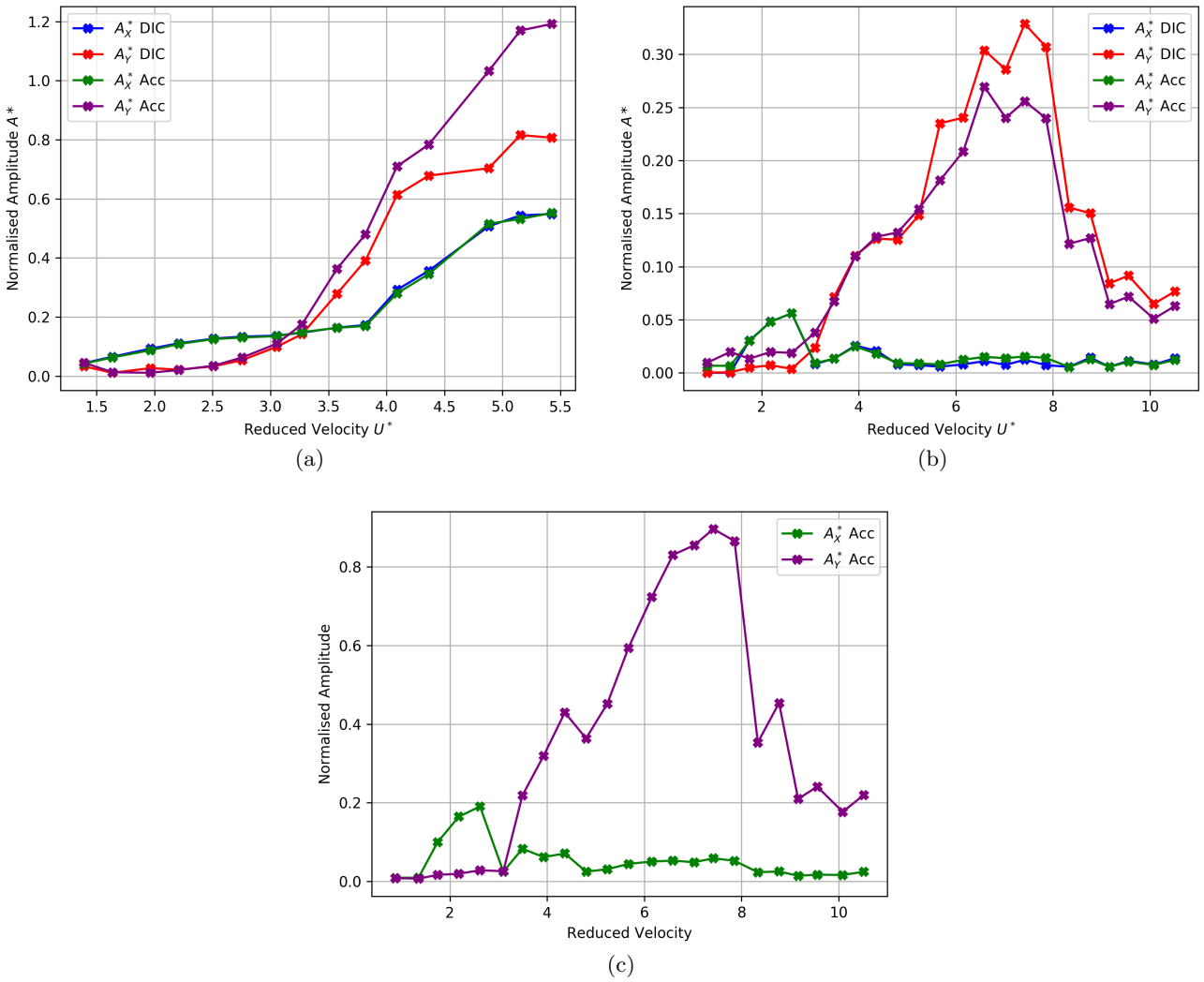

Figure 9: Normalised motion amplitudes vs. reduced velocity at Acc 1 of the fully submerged cylinder (a), at Acc 2 of the partially submerged cylinder (b) and at Acc 1 of the partially submerged cylinder (c)

The deviations between both measurement techniques have to be classified to assess the suitability of DIC for VIV. The deviation of small amplitudes ($A \leq 1\,\text{mm}$) results from a too coarse pattern and a wide field of view and therefore an insufficient spatial solution – compare [25].
With rising displacement amplitudes, results show that DIC and accelerometer techniques deliver almost identical results for amplitudes normal to the flow between 2.3 mm and 4.8 mm ($0.07 \leq A^* \leq 0.15$). For large amplitudes, the results differ strongly, which increases with rising displacement amplitudes. Generally, the results differ significantly less in flow direction (in-plane motion of the camera) compared to the normal direction of the flow (out-of-plane motion). Sutton et al. [26] investigated measurement errors resulting from out-of-plane motions. They concluded that for 3D DIC out-of-plane motions have no influence on the in-plane measurements. However, the error in out-of-plane direction increases linearly with the out-of-plane

transitional displacement. This explains why the deviation are significantly large in transverse direction but neglectable in longitudinal direction. Additionally, the time series in Figure 8c and those of higher flow velocities, which are not included in the present study, support this thesis, because, nevertheless the amplitudes differ, the time series are almost identical between the peaks. The deviation after the peak in Figure 9b may result from the increasing bending through static flow pressure but this is just an assumption and has to be investigated.

Figure 10 compares the dominant oscillation frequencies of both cylinders and methods. For the partially submerged cylinder, the longitudinal oscillation frequency rises when being in the stream wise branch, but remains constant afterwards. Additionally, a second much smaller peak exists when the longitudinal and transverse motions are not in resonance.

For the fully submerged cylinder, the longitudinal frequency follows the trend of the transverse frequency but doubles the longitudinal value. This phenomenon is typically for the lock-in region of structures exposed to VIV (Bearman [27]). Here, a second much smaller peak exists, when the transverse amplitude gets larger than the longitudinal amplitude.

DIC and accelerometer deliver always almost the same frequencies for both cylinders and all flow velocities and resulting amplitudes except when the longitudinal amplitude of the partially submerged cylinder is extremely low. This reflects the decay test results listed in Table 1.

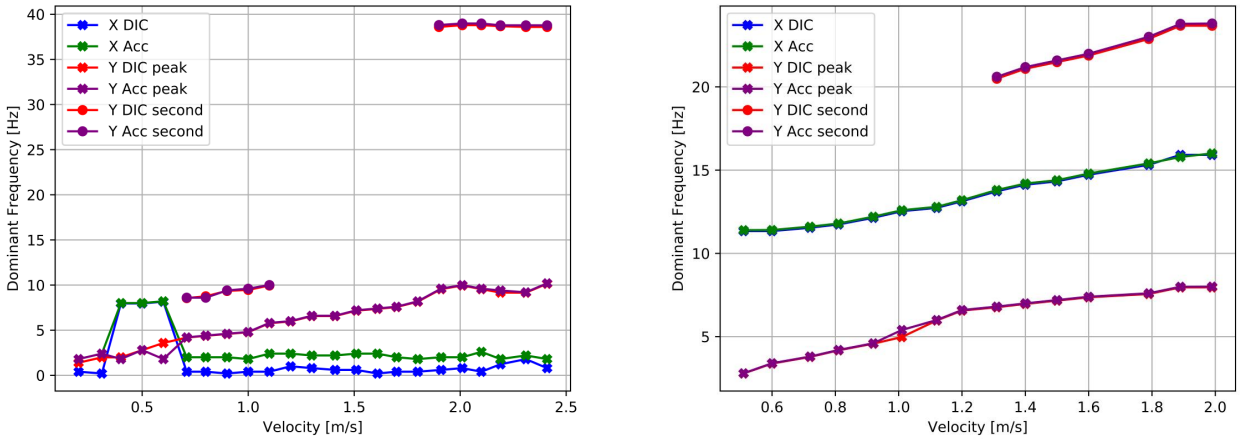

Figure 10: Dominant frequencies vs. velocity of (a) the partially submerged cylinder and (b) the fully submerged cylinder

4 CONCLUSION

Experimental investigations of fully and partially submerged cylinders exposed to VIV were carried out. Accelerations and displacements were measured comparatively using 3D accelerometer and 3D DIC measurement techniques. The motions amplitudes of the partially submerged cylinder indicate a wide range of resonance as well as a stream wise branch for flow velocities below resonance. For the fully submerged cylinder, the resonance region could be depicted partially due to limitation of the maximum flow velocity and structural failure of the test body under high VIV induced loads.

The comparison between DIC and accelerometer measured displacements show a fair agreement over a large range of flow velocities. For small displacements, a deviation between both measurement techniques result from the pattern coarseness and thus a lack in spatial resolution. For large displacements with high amplitudes both measurement techniques deviate. These deviations may be due to out-of-plane motion. Despite the deviations of amplitudes, the DIC and accelerometer measured frequencies in all degrees of

freedom were practically identical.
Summarising, the resulting in-plane motions, here motion in flow direction, detected with DIC and accelerometers, match well over the complete observed velocity range. In contrast, the motion normal to flow, out-of-plane motion, only matches for certain range of motion amplitudes. Therefore, DIC is generally suitable for VIV investigations. However, it is limited by the solvable out-of-plane amplitude. The lack of out-of-plane accuracy over a wide band of amplitudes, which is most important and characteristic for VIV, makes it still challenging to use DIC instead alternative techniques. Thus, future investigations will focus on out-of-plane motions and accuracy as well as the camera arrangement. If the focus of an VIV investigation lies on frequencies instead of amplitudes DIC may be used without limitations.

5 ACKNOWLEDGEMENTS

The authors are grateful to LaVision and especially to Mr. Mannel for the permission to use the software DaVis 10 with the module StrainMaster [22] to carry out the present study.

REFERENCES

[1] R. Prastianto, K. Otsuka and Y. Ikeda. "Vortex-induced vibration of a flexible free-hanging circular cantilever". In: *ITB Journal of Engineering Science* 41 (2009), pp. 111–125.

[2] A. Khalak and C. Williamson. "Dynamics of a hydroelastic cylinder with very low mass and damping". In: *Journal of Fluids and Structures* 10.5 (1996), pp. 455–472.

[3] A. Khalak and C. Williamson. "Fluid forcs and dynamics of a hydroelastic structure with very low mass and damping". In: *Journal of Fluids and Structures* 11.8 (1997), pp. 973–982.

[4] A. Khalak and C. Williamson. "Investigation of relative effects of mass and damping in vortex-induced vibration of a circular cylinder". In: *Journal of Wind Engineering and Industrial Aerodynamics* 69-71 (1997). Proceedings of the 3rd International Colloqium on Bluff Body Aerodynamics and Applications, pp. 341–350.

[5] A. Khalak and C. Williamson. "Motions, forces and mode transitions in vortex-induced vibrations at low mass-damping". In: *Journal of Fluids and Structures* 13.7 (1999), pp. 813–851.

[6] A. Fujarra, C. Pesce, F. Flemming and C. Williamson. "Vortex-induced vibration of a flexible cantilever". In: *Journal of Fluids and Structures* 15 (2001), pp. 651–658.

[7] R. W. Prastianto, K. Otsuka and Y. Ikeda. "Hydrodynamic forces on multiple free-hanging circular cantilevers in uniform flows". In: *International Journal of Offshore and Polar Engineering* 19 (2009), pp. 108–114.

[8] X. Wang, Z. Hao and S. Tan. "Vortex-induced vibrations of a neutrally buoyant circular cylinder near a plane wall". In: *Journal of Fluids and Structures* 39 (2013), pp. 188–204.

[9] X. Wang, C. Wang, Y. Li and S. Tan. "Flow patterns of a low mass-damping cylinder undergoing vortex-induced vibration: Transition from initial branch and upper branch". In: *Applied Ocean Research* 62 (2017), pp. 89–99.

[10] N. Shaharuddin and I. Darus. "Experimental study of vortex-induced vibrations of flexibly mounted cylinder in circulating water tunnel". In: *Acta Mechanica* 226.11 (2015), pp. 3795–3806.

[11] C. Williamson and R. Govardhan. "Vortex-induced vibrations". In: *Annual Review of Fluid Mechanics* 36.1 (2004), pp. 413–455.

[12] C. Williamson and R. Govardhan. “A brief review of recent results in vortex-induced vibrations”. In: *Journal of Wind Engineering and Industrial Aerodynamics* 96.6 (2008). 5th International Colloquium on Bluff Body Aerodynamics and Applications, pp. 713–735.

[13] T. Sarpkaya. “A critical review of the intrinsic nature of vortex-induced vibrations”. In: *Journal of Fluids and Structures* 19.4 (2004), pp. 389–447.

[14] X. Wu, F. Ge and Y. Hong. “A review of recent studies on vortex-induced vibrations of long slender cylinders”. In: *Journal of Fluids and Structures* 28 (2012), pp. 292–308.

[15] M. Helfrick, C. Niezrecki, P. Avitabile and T. Schmidt. “3D digital image correlation methods for full-field vibration measurement”. In: *Mechanical systems and signal processing* 25.3 (2011), pp. 917–927.

[16] Z. Tang, J. Liang, Z. Xiao and C. Guo. “Large deformation measurement scheme for 3D digital image correlation method”. In: *Optics and lasers in engineering* 50.2 (2012), pp. 122–130.

[17] J. Banks, L. Giovannetti, X. Soubeyran, A. Wright, S. Turnock and S. Boyd. “Assessment of digital image correlation as a method of obtaining deformations of a structure under fluid load”. In: *Journal of Fluids and Structures* 58 (2015), pp. 173–187.

[18] R. Bleischwitz, R. de Kat and B. Ganapathisubramani. “Near-wake characteristics of rigid and membrane wings in ground effect”. In: *Journal of Fluids and Structures* 80 (2018), pp. 199–216.

[19] S. Gupta, V. Parameswaran, M. Sutton and A. Shukla. “Study of dynamic underwater implosion mechanics using digital image correlation”. In: *Proceedings of the Royal Society A: Mathematical, Physical and Engineering Sciences* 470.2172 (2014), p. 20140576.

[20] F. Hild and S. Roux. “Digital image correlation: from displacement measurement to identification of elastic properties–a review”. In: *Strain* 42.2 (2006), pp. 69–80.

[21] B. Pan, K. Qian, H. Xie and A. Asundi. “Two-dimensional digital image correlation for in-plane displacement and strain measurement: a review”. In: *Measurement science and technology* 20.6 (2009), p. 062001.

[22] LaVision. *StrainMaster - Digital Image Correlation Systems for Full Field Shape, Displacement and Strain*. 2019. URL: `https://www.lavision.de/en/download.php?id=323`.

[23] N. Jauvtis and C. Williamson. “Vortex-induced vibration of a cylinder with two degrees of freedom”. In: *Journal of Fluids and Structures* 17.7 (2003), pp. 1035–1042.

[24] N. Jauvtis and C. Williamson. “The effect of two degrees of freedom on vortex-induced vibration at low mass and damping”. In: *Journal of Fluid Mechanics* 509 (2004), pp. 23–62.

[25] LaVision. *DIC Tips and Tricks in DaVis*. 2016.

[26] M. Sutton, J. Yan, V. Tiwari, H. Schreier and J.-J. Orteu. “The effect of out-of-plane motion on 2D and 3D digital image correlation measurements”. In: *Optics and Lasers in Engineering* 46.10 (2008), pp. 746–757.

[27] P. Bearman. “Vortex shedding from oscillating bluff bodies”. In: *Annual review of fluid mechanics* 16.1 (1984), pp. 195–222.